EFFECTS OF LAYER INTERFACE SLIP ON THE RESPONSE AND PERFORMANCE OF ELASTIC MULTI-LAYERED FLEXIBLE AIRPORT PAVEMENT SYSTEMS

James W Maina*[1], Morris De Beer[1], and Kunihito Matsui[2]
*[1]CSIR Built Environment, P.O. Box 395
Pretoria 0001, South Africa
JMaina@csir.co.za
[2]Tokyo Denki University, Saitama, Japan

Abstract: The new AASHTO Pavement design guide for flexible pavements is shifting from an experience (or purely empirical) based design method to a mechanistic-empirical (M-E) design method. The latter approach requires an elastic multilayered analysis to compute responses of interest and use empirically established models to determine airport pavement distresses like fatigue cracking of asphalt concrete layer and as well as rutting or plastic deformation.

Three different types of compliance models that simulate pavement layer interface slip and introduced into the multilayered elastic analysis freeware known as GAMES are presented in this paper. The GAMES software is capable of analyzing effects of five different types of airport pavement surface loading, namely; vertical, horizontal (shear), torsion, moment and centripetal forces. Airport pavement responses due to multiple loadings are determined by using the superposition concept applicable to linear elastic theory, where responses from each wheel load are decomposed into the x-y-z components before summing-up the responses at each point.

In this study, the effect of layer interface slip rate on the critical responses such as (primary) tensile strains as well as strain distortion energies for a flexible runway pavement structure is examined based on strain energy of distortion. The strain energies have, in recent years, received attention as an indication of potential fatigue and/or damage failure criteria. Important environmental effects such as pavement moisture and temperature were, however, not analytically considered in this study.

INTRODUCTION

Governing Equations for Pavement Response

Pavement is assumed to be composed of n layers parallel to each other and the bottom layer (n^{th} layer) is semi-infinite. It is convenient to use a cylindrical coordinate system (r,z), when the problem is axi-symmetric where the vertical load is applied at the surface and is uniformly distributed over a circle of radius a. If u_r and u_z are displacement components in r- and z-directions, respectively, the governing equations can be written as,

$$\nabla^2 u_r + \frac{1}{1-2\nu}\frac{\partial}{\partial r}\left(\frac{\partial u_r}{\partial r}+\frac{u_r}{r}+\frac{\partial u_z}{\partial z}\right)-\frac{u_r}{r^2}=0 \qquad (1)$$

$$\nabla^2 u_z + \frac{1}{1-2\nu}\frac{\partial}{\partial z}\left(\frac{\partial u_z}{\partial z} + \frac{u_r}{r} + \frac{\partial u_r}{\partial r}\right) = 0 \tag{2}$$

where, ν is a Poison's ratio and ∇^2 is the Laplace operator given as[4]:

$$\nabla^2 = \frac{\partial^2}{\partial r^2} + \frac{1}{r}\frac{\partial}{\partial r} + \frac{\partial^2}{\partial z^2} \tag{3}$$

Boundary conditions of the problems can be given as shown in Eqs. (4), since the surface loading is uniformly distributed over a circular area.

When $r \le a$

$$\sigma_z(r,0) = -p, \quad \tau_{rz}(r,0) = 0 \tag{4a}$$

and when $r > a$

$$\sigma_z(r,0) = \tau_{rz}(r,0) = 0 \tag{4b}$$

When a horizontal surface load is considered, the problem becomes asymmetric. In this case, the governing equations can be expressed as:

$$\nabla^2 u_r + \frac{1}{1-2\nu}\frac{\partial}{\partial r}\left(\frac{\partial u_r}{\partial r} + \frac{u_r}{r} + \frac{1}{r}\frac{\partial u_\theta}{\partial \theta} + \frac{\partial u_z}{\partial z}\right) - \frac{u_r}{r^2} - \frac{2}{r^2}\frac{\partial u_\theta}{\partial \theta} = 0 \tag{5}$$

$$\nabla^2 u_\theta + \frac{1}{1-2\nu}\frac{1}{r}\frac{\partial}{\partial \theta}\left(\frac{\partial u_r}{\partial r} + \frac{u_r}{r} + \frac{1}{r}\frac{\partial u_\theta}{\partial \theta} + \frac{\partial u_z}{\partial z}\right) - \frac{u_\theta}{r^2} - \frac{2}{r^2}\frac{\partial u_r}{\partial \theta} = 0 \tag{6}$$

$$\nabla^2 u_z + \frac{1}{1-2\nu}\frac{\partial}{\partial z}\left(\frac{\partial u_r}{\partial r} + \frac{u_r}{r} + \frac{1}{r}\frac{\partial u_\theta}{\partial \theta} + \frac{\partial u_z}{\partial z}\right) = 0 \tag{7}$$

in which, ν a Poisson's ratio, and ∇^2 is the Laplace operator given as:

$$\nabla^2 = \frac{\partial^2}{\partial r^2} + \frac{1}{r}\frac{\partial}{\partial r} + \frac{1}{r^2}\frac{\partial^2}{\partial \theta^2} + \frac{\partial^2}{\partial z^2} \tag{8}$$

u_r, u_θ and u_z are displacement components in the directions of cylindrical coordinate axes (r, θ, z). Boundary conditions at the surface are as follows:

When $r \le a$

$$\tau_{rz} = -q\cos\theta, \quad \tau_{\theta z} = q\sin\theta, \quad \sigma_z = 0 \tag{9a}$$

and when $r > a$

$$\tau_{rz} = \tau_{\theta z} = \sigma_z = 0 \tag{9b}$$

If one solves Eqs. (1) and (2) with boundary conditions presented in Eq. (4), axi-symmetric solutions can be obtained. Also, by solving Eqs. (5) ~ (7) with boundary conditions from Eq. (9) asymmetric solutions are obtained. Details of the derivation of the solutions are explained elsewhere (Maina and Matsui, 2004). When both vertical and horizontal forces act at the surface, responses from individual loads are computed first and then superimposed to obtain the final results. Positive sign refers to tension, while negative sign refers to compression.

Layer Interface Condition

One of the factors affecting performance of in-service airport pavements is the condition at layer interfaces. Pavement sections like runways and small radius curves are prone to layer de-bonding because of the presence of high horizontal loading. Layer de-bonding results the redistribution of stresses and strains in the pavement structure, causing premature pavement failures. In this study, slip compliance models were introduced into the general analytical process in an attempt to get a better understanding of the behavior of pavement structures under the action of vertical and horizontal loadings for cases with layer interface slip.

Interface Slip Models

A Coulomb type model is often used to express an interface slip (Huang, 2004). However, since the model results in nonlinear problem, it is difficult to derive analytical solutions with an interface slip. The software BISAR developed in 1973 (De Jong *et al*, 1979) introduced a compliance model, and a similar concept is also utilized in this study. When a slip takes place at the interface between i^{th} and $(i+1)^{th}$ layers, the phenomenon is modeled as,

$$(1-\alpha_i)\left\{u_r^i(h_i) - u_r^{i+1}(0)\right\} = \alpha_i \beta_i \tau_{rz}^i(h_i) \tag{10}$$

in which, α_i is called a slip rate. Complete bonding is represented by $\alpha_i = 0$, while if α_i approaches 1, the interface condition becomes nearly perfect slip. $\tau_{rz}^i(h_i)$ is shearing stress at the interface between i^{th} and $(i+1)^{th}$ layers. Eqs. (11) ~ (13) represent the three models for β_i that are considered in this study, such that α_i becomes a dimensionless parameter.

$$\text{Slip Model 1}: \beta_i = b^* \left(\frac{1+\nu_i}{E_i} + \frac{1+\nu_{i+1}}{E_{i+1}} \right) \tag{11}$$

$$\text{Slip Model 2}: \beta_i = 2b^* \left(\frac{1+\nu_i}{E_i} \right) \tag{12}$$

$$\text{Slip Model 3}: \beta_i = 2b^* \sqrt{\left(\frac{1+\nu_i}{E_i} \right)\left(\frac{1+\nu_{i+1}}{E_{i+1}} \right)} \tag{13}$$

b^* must have a unit of length in order for α_i to be dimensionless. Thus b^* is selected as a maximum radius among the surface loadings.

Eq. (11) is the model, which shows the arithmetical means of inverted shear moduli of i^{th} and $(i+1)^{th}$ layers. Eq. (12) uses only the inverted shear modulus of upper layer, while Eq. (13 shows the geometric mean of inverted shear moduli between i^{th} and $(i+1)^{th}$ layers. These models were incorporated into GAMES software using a procedure explained by Maina and Matsui (2004).

Strain Energy of Distortion (SED)

According to Timoshenko and Goodier (1951), the quantity of strain energy stored per unit volume of the material can be used as a basis for determining the limiting stress at which failure occurs. For this, to be applied to isotropic materials, it is important to separate this energy into two parts; one due to the change in volume and the other due to the distortion, and consider only the second part in determining the strength. Whatever the stress system, failure occurs when the strain energy of distortion reaches a certain limit. Now, total strain energy per unit volume, V_0, can be expressed by using Hooke's law as follows:

$$V_0 = \frac{1}{2E}\left(\sigma_x^2 + \sigma_y^2 + \sigma_z^2\right) - \frac{\nu}{E}\left(\sigma_x\sigma_y + \sigma_y\sigma_z + \sigma_z\sigma_x\right) + \frac{1}{2G}\left(\tau_{xy}^2 + \tau_{yz}^2 + \tau_{xz}^2\right) \qquad (15)$$

Whereas the strain energy due to distortion, *SED*, can then be expressed as follows:

$$SED = V_0 - \frac{1-2\nu}{6E}\left(\sigma_x + \sigma_y + \sigma_z\right)^2 \qquad (16)$$

Using the above equations, it is anticipated that points within the pavement structural system that have higher values of strain energy of distortion (SED) will potentially fail first before points with relatively lower values, as was also indicated by Perdomo and Nokes (1993).

Worked Examples

The three slip models introduced earlier were used in the analysis in order to evaluate their influence on the airport pavement. The following six values of slip ratio: 0.0, 0.2, 0.4, 0.6, 0.8 and 0.9 were used where 16 wheels of a Boeing-747-400 were assumed to act on the surface of the pavement structural model whose cross section is shown in Table 1. The wheel diameter of 45.8 cm and loading of 227.5 kN for vertical and 113.75 kN for horizontal were used.

Table 1 Five Layer Airport Pavement Model – (this study)

Layer	Thickness (cm)	Modulus (MPa)	Poisson's ratio
Asphalt concrete	5	2,000	0.44
Asphalt base	8	2,250	0.44
Asphalt treated base	15	2500	0.44
Stabilized crushed aggregate base	23	1000	0.35
Subgrade soil	∞	200	0.40

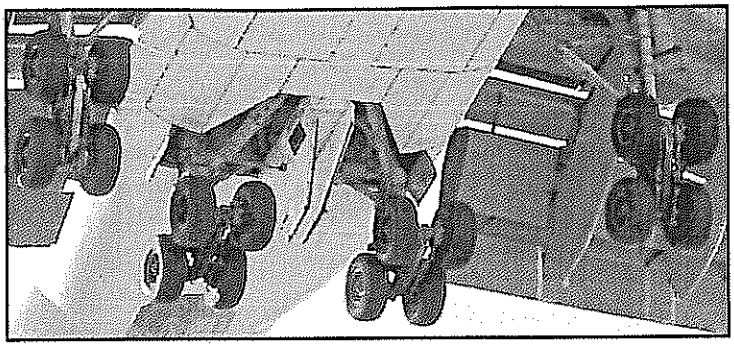

Figure 1: Boeing 747-400 Wheel Load configuration used in this study

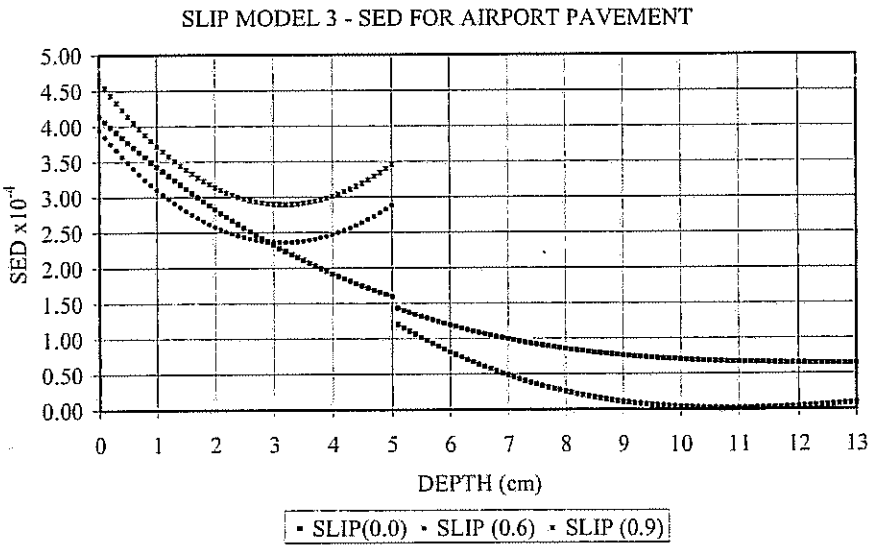

Figure 2: Variation of SED from Slip Model 3 with depth - Vertical and Horizontal Tyre Loading

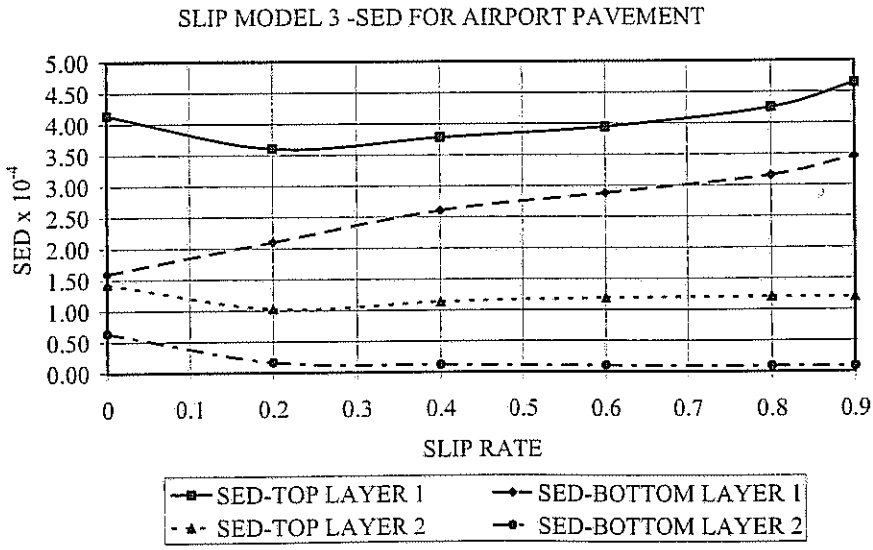

Figure 3: Variation of SED with Slip Rate (Slip Model 3) at layer boundaries - Vertical and Horizontal Tyre Loading

OBSERVATIONS AND DISCUSSIONS

For the purpose of this paper the results of only Slip Model 3 are discussed. Figure 2 show the variation of SED with depth for three slip rate values using Slip Model 3 (Eq 13). The trend of SED indicates that for whatever the slip rate value, higher SED values are found to be at the surface of the pavement structure. As the slip rate increases, SED at the bottom of the top layer (where the interface slip occurs) increases to almost 75 per cent of the SED at the top of the pavement and this may further result in a potential bottom-up failure condition. This also occurred for the other two slip models, but less with a lesser sensitivity. Based on SED analysis, interlayer slip as discussed here may therefore influence the position and type of potential asphalt layer failures such as cracking and deformation. Less drastic changes in SED occurred in bottom Layer 2. The general trend in SED with depth in Figure 2 indicate that as the slip rate increases SED tend to decrease up to a certain point (in this particular case slip rate = 0.2) and then start increasing again. Figure 3 illustrates the variation in SED with pavement depth, at three slip rates and it is clear that a redistribution of stresses and strains (as defined by the SED) occurs, especially in the 5 cm layer at the top (i.e. Layer 1). The SEDs peaked both at the top and bottom of this layer, suggesting potential damage (i.e. cracking, detoriation) from both the top and bottom of Layer 1 under vertical and horizontal aircraft loading (i.e. cornering).

A recent pavement failure at an international airport in South Africa handling almost 3 million passengers annually, where 8 m of the top asphalt layer debonded, resulted in a delay of almost 6 hours causing flights to be diverted to other local airports (The Star, 2005). The procedure given above might be used to estimate the effect of layer interface conditions in asphalt pavements beforehand, which could enable more accurate risk determination for these airport pavements. Further research in this area is continuing.

ACKNOWLEDGMENTS

The CSIR Built Environment Unit and the Centre for High Performance Computing (CHPC) at Meraka Institute of the CSIR are thanked for their support during this study.

REFERENCES

De Jong, D. L., Peutz, M. G. F. & Korswargen, A. R. (1979). BISAR, External Report AMSR.0006.73, Koninklijke/Shell-Laboratorium, Amsterdam, 1979.

Huang, Y. H. (2004). *Pavement Analysis and Design.* Pearson Prentice Hall, NJ.

Maina, J. W. & Matsui, K. (2004). Developing software for elastic analysis of pavement structure responses to vertical and horizontal surface loadings. *Transportation Research Record, 1896*, 107-118.

The Star, www.thestar.co.za, Article dated November 28, 2005.

Timoshenko, S. & J. N. Goodier. (1951). *Theory of Elasticity*. New York: McGraw-Hill Book Company, Inc.

Perdomo, D. & Nokes, B. (1993). Theoretical Analysis of the effects of Wide-Base Tires on Flexible Pavements using CIRCLY. *Transportation Research Record, 1388*, 108-119.